

# The Effects of Background Pressure on SPT-140 Hall Thruster Performance

John Steven Snyder\*

*Jet Propulsion Laboratory, California Institute of Technology, Pasadena, CA, 91109*

Giovanni Lenguito†

*SSL, Palo Alto, CA, 94303*

Jason D. Frieman,‡ Thomas W. Haag,§ and Jonathan A. Mackey\*\*

*NASA Glenn Research Center, Cleveland, OH, 44135*

NASA's planned Psyche mission is scheduled to launch in 2022 and begin a 3.5-year cruise to the metallic asteroid Psyche, where it would examine this unique body. The baseline spacecraft design is a hybrid of JPL's deep-space heritage subsystems with commercial partner SSL's power, structure, and SPT-140 electric propulsion subsystems. Since the deep-space implementation of the SPT-140 differs from the commercial implementation, primarily in the need for deep power throttling, characterization of the system at lower powers is necessary. One specific area of interest is the sensitivity of thruster performance to background pressure in ground-based test facilities, which can have an impact on the prediction of in-space performance. Measurements of this pressure dependence were performed on a qualification-model SPT-140 thruster over the 0.9-4.5 kW range of interest for the Psyche mission. Thrust sensitivity to pressure, in an absolute sense, was largest at 4.5 kW and decreased with power until there was little-to-no measurable effect at 0.9 kW. In a relative sense, thrust sensitivity was similar at all powers above 0.9 kW with about 2-4% higher thrust measured at 10  $\mu$ Torr than at the lowest operating pressure. Thruster magnetic field sensitivity, examined as a function of magnet current, did not have a strong dependence on facility pressure. Finally, an investigation of low-power operation at the lowest facility pressure showed that a combination of added cathode keeper current and additional cathode propellant flow significantly mitigated the larger negative cathode-to-ground voltages that were observed. These test results, combined with thruster life test results, inform the selection of proper low-power operating conditions for Psyche.

## I. Introduction

Psyche is a planned NASA Discovery mission to rendezvous with and orbit the asteroid Psyche, a body unlike any other in the solar system. An asteroid composed almost entirely out of metal, Psyche could be the bare core of a planetesimal that was stripped of its mantle during collisions early in solar system formation, or perhaps composed of primordial metal-rich materials that accreted closer to the sun. It is an exciting target and ripe for scientific exploration. The mission to Psyche, which orbits the sun near 3 AU, will rely on a Mars gravity assist and electric propulsion for the heliocentric cruise from Earth.<sup>1</sup> Once at the asteroid, electric propulsion will also be used to transfer between the various science orbits and for orbit maintenance. The spacecraft will carry no chemical propulsion system.

The Psyche spacecraft is a hybrid of systems provided by JPL and its commercial partner SSL.<sup>2</sup> SSL has extensive experience in both electric propulsion and high-power spacecraft, and this is combined with JPL's heritage in deep-space command and data handling hardware, telecommunications hardware, and flight software. The resulting design

---

\* Senior Engineer, Electric Propulsion Group, [steve.snyder@jpl.nasa.gov](mailto:steve.snyder@jpl.nasa.gov), Associate Fellow AIAA.

† Propulsion Development Engineer, Propulsion Group, [giovanni.lenguito@sslmda.com](mailto:giovanni.lenguito@sslmda.com).

‡ Research Engineer, Electric Propulsion Systems Branch, [jason.d.frieman@nasa.gov](mailto:jason.d.frieman@nasa.gov), Member AIAA.

§ Research Engineer, Electric Propulsion Systems Branch, [thomas.w.haag@nasa.gov](mailto:thomas.w.haag@nasa.gov), Member AIAA.

\*\* Research Engineer, Electric Propulsion Systems Branch, [jonathan.a.mackey@nasa.gov](mailto:jonathan.a.mackey@nasa.gov), Member AIAA.

reduces implementation risk by preserving the core capabilities of each organization and by simplifying and controlling interfaces between systems.

Psyche would use SSL’s SPT-140 electric propulsion system. It is based on the SPT-100 subsystem that SSL has been successfully flying for over a decade,<sup>3</sup> and will first launch on an SSL spacecraft in mid-2018. The commercial implementation of the SPT-140 system is modeled on an electric orbit-raising phase with the thruster operating at a full discharge power of 4.5 kW, followed by a station-keeping phase at a reduced power of 3.0 kW.<sup>4,5</sup> The system design, and the thruster development, were derived from this nominal operations plan. Psyche, however, will have to operate at up to 3.3 AU from the sun at a much wider range of powers.

An example of thruster operating durations and powers is shown in Fig. 1 for a candidate cruise trajectory. The spacecraft will use only a single thruster at a time. Most thrusting is done at a full discharge power of 4.5 kW, until the heliocentric distance becomes such that throttling is necessary; the lowest power that is necessary during cruise is about 2.0 kW. Orbital transfers and other operations at the asteroid (i.e. proximity operations) are performed at a discharge power of 1.0 kW. Four thrusters are available on the spacecraft, but single-fault tolerance requirements mean the mission must be able to be completed with only three.

Prior to selection of the Psyche mission for the Discovery program, a series of detailed tests and analyses were performed to examine the performance, operability, and lifetime of the SPT-140 thruster over a range of conditions and scenarios applicable to deep-space missions. The first test program investigated the performance and operation of the Development Model 4 (DM4) thruster at discharge powers of 0.23 kW to 6.0 kW, and observed stable operation and performance over this range.<sup>6</sup> A notable finding was that at powers below 1.5 kW the cathode-to-ground voltage became increasingly negative, and that this was mitigated with the addition of steady-state keeper current and also additional propellant flow to the cathode. The second test program repeated many of the same measurements on the flight-model Qualification Model 2 (QM002) thruster with similar results.<sup>7</sup> In addition, this thruster was successfully operated at 0.8 kW for a duration of 27 hours to assess the operational stability at low power. Supplemental tests included plasma probe measurements to gather data for numerical simulations, and an integrated test with a thruster and a modified SSL Power Processing Unit (PPU) capable of operating a different xenon flow control valve (this valve was necessary to achieve the required throttleability over the full range of power for Psyche). Finally, the SPT-140 life test was extended by operating the life test unit (QM001) at discharge powers of 0.9 and 1.0 kW for 250 hours each.<sup>4</sup> There was no indication of performance anomalies or lifetime impacts due to operation at low powers.

Many Hall thrusters, but not all, exhibit a measurable performance dependence on the test facility background pressure.<sup>8-13</sup> This dependence is thought to be related to electron transport in the near-field region of the thruster plume, but the specific mechanisms have not yet been identified.<sup>11</sup> This is a particularly important issue for flight implementation since mission design and operations rely on accurate thrust predictions, and existing Hall thruster test facilities cannot achieve the very low pressures of the space environment. If a trajectory is designed using a certain thrust level that is ultimately not realized in space, this could put a mission at risk of successful completion. As such, it is necessary to be able to correct ground-test data for this pressure dependency to accurately predict in-space performance.

As an example of this effect, investigation of the SPT-100 thruster performance as a function of facility background pressure has shown a modest ~3 mN (4%) increase in measured thrust at full power as pressure was increased from 1.7 to 70  $\mu$ Torr (i.e. a factor of 40).<sup>8</sup> Most of that pressure dependence occurred at pressures between 5 and 20  $\mu$ Torr, and the data suggest that there may be little pressure dependence below 5  $\mu$ Torr. In spite of this dependence, in-orbit estimates of thrust on SSL spacecraft have shown good agreement with ground test data.<sup>14</sup> SSL has also characterized the performance of the SPT-140 as a function of facility background pressure as a part of its system development, but this characterization was done only at the 3.0 and 4.5 kW operating points planned for commercial satellites and those data have not been published.

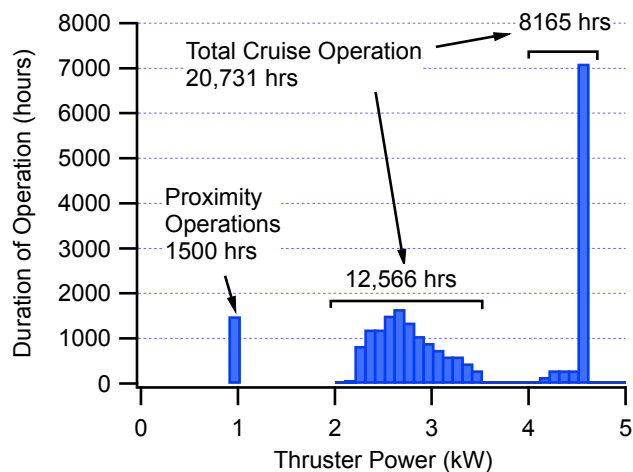


**Fig. 1. Histogram of EP System Operating Duration for a Candidate Psyche Trajectory.**

The motivation for the work described in this paper is twofold: first, to characterize the performance of the SPT-140 thruster as a function of background pressure over the range of powers expected to be used by the Psyche mission, in order to gather the data necessary for predicting the in-space performance; and second, to gather additional data on low-power operation to inform the selection of mission operating conditions and revision of hardware performance requirements where necessary. It is important to conduct these tests in facilities that can obtain low pressures which approximate the vacuum of space, to reduce the uncertainties in prediction of in-space performance. Psyche mission partner NASA Glenn Research Center (GRC) has the premier facility in the country for these types of measurements, with pumping speeds of up to 700 kL/s and a no-load pressure of 0.1  $\mu$ Torr.

## II. Test Setup and Methods

### A. SPT-140 Thruster and Thruster Auxiliary Support Unit (TASU)

The SPT-140, shown in Fig. 2, is a mid-power-class Hall thruster produced by Fakel EDB (Kaliningrad, Russia). The thruster consists of four main components: an annular anode and discharge channel, an external cathode, and an internal magnetic circuit consisting of electromagnet coils and pole structure. Ample description of the physics of the Hall thruster can be found in literature,<sup>15</sup> therefore this section is limited to the characteristic features of the SPT-140.

The anode unit hosts the ionization of the propellant of choice (xenon in the specific case) in the discharge channel that is made of an assembly of multiple ceramics (i.e. borosil and high-purity grade boron nitride)<sup>5</sup> and accelerates the ionized gas to produce thrust. The propellant is injected homogeneously from a stainless steel ring at the base of the discharge channel which also functions as the electrical anode, set to +300V with respect to the cathode during operation. The radial magnetic field is generated by a separate circuit that consists of one inner and one outer coil connected in series, which surround the inner pole and the discharge chamber respectively. Ionization is achieved by the collision of the neutral propellant atoms with electrons that move azimuthally in the discharge channel due to Lorentz forces. Finally, at the exit plane of the discharge channel the electric field accelerates the ionized atoms and generates thrust.

The cathode contains a lanthanum hexaboride (LaB<sub>6</sub>) thermionic emitter that releases the electrons needed to both ionize the propellant and neutralize the ionized beam after it is accelerated downstream of the thruster. This type of cathode uses a coiled resistive heat source to initially reach the temperature needed to activate the LaB<sub>6</sub> emitter; however, once the discharge between anode and cathode is initiated, the heater supply is turned off because the LaB<sub>6</sub> emitter is able to sustain itself. In order to initiate the discharge, the cathode of the SPT-140 includes an igniter electrode that generates a localized discharge via a high voltage ( $\sim 320$  V) pulse train produced by the SSL PPU. Moreover, the igniter electrode can be used as a keeper, whereby a steady-state current is drawn from the cathode to help sustain the thruster discharge at low power levels. The recommended maximum keeper power is 40 W; under the conditions examined in this test that limited the keeper current to approximately 1.75 A. Note an SSL PPU was not used to perform these tests, so laboratory power supplies with a steady DC voltage output were used to ignite the cathode and thruster.

The SPT-140 used for this test was the QM002 thruster that is identical to the qualification model thruster QM001 that went through formal qualification testing.<sup>4,5</sup> The QM002 unit was built specifically for the ancillary tests needed to verify the operation of the thruster at the system level and in various novel operation modes, as in the specific case of the Psyche mission. Therefore the QM002 design is fully qualified<sup>5</sup> and is representative of the flight models that are going to be built for the deep space mission. Only minor changes to improve manufacturability (e.g. a locking mechanism) have been reported since the fabrication of QM002, but those do not impact the operation, performance and life expectancy of the thruster.

The QM002 had already been subjected to a multitude of tests prior to the test program described here:<sup>5</sup> to understand the erosion pattern due to plume impingement on surfaces such as quartz; to characterize the emitted plume using diagnostics from various facilities; to characterize facility effects on the thruster performance; thermal balance

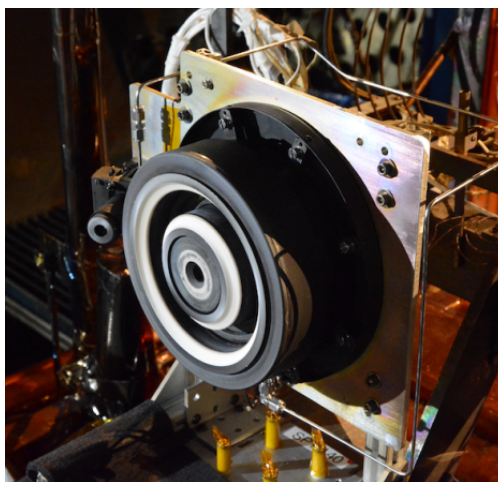


**Fig. 2. SPT-140 Qualification Model Thruster (QM002).**

tests; end-to-end tests including the complete SSL power distribution system; and electromagnetic compatibility tests. The thruster accumulated about 790 hours of operation during these tests, most of which was at powers of 3.0 and 4.5 kW, and about 320 hours of which was at powers greater than 3.8 kW. Because the discharge channel ceramic erodes and the thrust decreases over the first ~2000 hours of thruster life,<sup>5</sup> the performance data collected here will not be that of a beginning-of-life nor an end-of-life thruster. Thruster performance models for the Psyche mission will have to account for this.

The commercial implementation of the SSL SPT-140 system uses a Xenon Flow Controller (the XFC-140), also manufactured by Fakel EDB, that is tailored for the flow rates of the SPT-140 needed to operate in the range of 3.0 to 4.5 kW. This unit controls the total flow rate by means of a thermothrottle and guarantees the proper flow split between anode and cathode ( $\dot{m}_a : \dot{m}_c = 20 : 1$ , i.e. 5% cathode flow fraction) via a set of orifices. The XFC-140, however, does not have the dynamic range necessary to provide the flow rates needed for the low power thruster operation. A new xenon flow controller design will be implemented on Psyche that can operate over the range of powers required for the mission. For this test, the laboratory flow controllers described in Section II.B were used to control the xenon flow rates.

The SPT-140 flight system contains an additional unit called the Thruster Auxiliary Support Unit (TASU-140) which provides system cross-strapping features, ground-test features, and electrostatic discharge protection. It also houses the discharge filter capacitor for the system (a filter inductor is housed in the PPU). The passive LC filter attenuates the normal thruster plasma discharge oscillations, usually peaking in the frequency range of 20 kHz to 40 kHz, between the power supplies and the thruster. The unit is configured in a way that provides full isolation of the circuitry; the anode and cathode can therefore float with respect to ground, which is the configuration of choice for the tests presented in this manuscript. An engineering model TASU-140 was implemented in this test along with a spare PPU filter inductor to provide a flight-like discharge power circuit.

## B. Test Facility and Instrumentation

All experiments detailed in this work were performed in Vacuum Facility 5 (VF-5) at the NASA Glenn Research Center (GRC). VF-5 is a cylindrical chamber measuring 4.6 m in diameter and 18.3 m in length.<sup>16</sup> For this test, VF-5 was evacuated using a series of cryopumps. The cryopumps have a total effective pumping area of 33.5 m<sup>2</sup> and a combined nominal pumping speed of approximately 700 kL/s on xenon.<sup>16-18</sup> In order to obtain the lowest possible background pressure, the SPT-140 was installed in the main volume of VF-5 at the same location previously used to perform facility effects characterization tests on the NASA Hall Effect Rocket with Magnetic Shielding (HERMeS).<sup>19</sup> The placement of the cryopumps relative to the thruster at this location as well as the resultant near-field background neutral distribution is described in previous work.<sup>16-18</sup>

Facility pressure was monitored with two xenon-calibrated Bayard-Alpert style hot-cathode ionization gauges. The first (IG#2) has a downstream-facing orifice and was mounted on a boom arm at a location approximately 1.08 m radially outward from the centerline of the SPT-140, as shown in Fig. 3. The second (IG#3) was located approximately 0.7 m radially outward and centered approximately 0.08 m upstream of the thruster exit plane. The orifice of IG#3 faced radially outward (i.e., away from the thruster). Both gauges were configured to be compliant with all guidelines

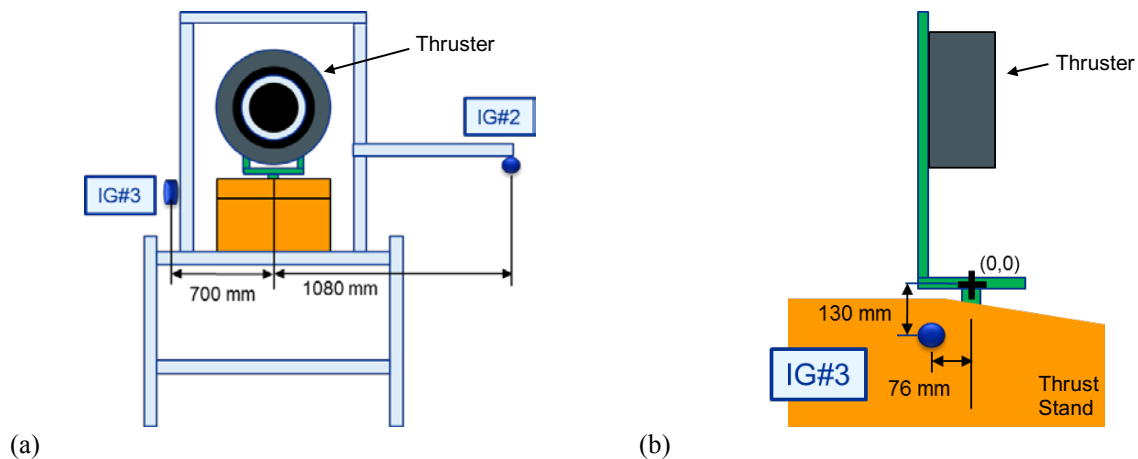


Fig. 3. (a) Front and (b) Side View Schematic of the Internal Ion Gauge Configuration (not to scale).

described in the recommended practices for pressure measurements in electric propulsion testing.<sup>20</sup> Consistent with previous facility effects tests performed in VF-5, all pressures reported in this work correspond to the measurements made using IG #3.<sup>9,19</sup>

Xenon propellant was supplied to the thruster anode and cathode using a laboratory feed system composed of stainless-steel lines metered with commercial thermal mass flow controllers. The anode line was metered using a 200 sccm controller and the cathode line was metered using a 100 sccm controller. An additional line, metered by a 2000 sccm controller, was used to inject xenon into the facility a few meters downstream of the thruster in order to modulate facility pressure. All flow controllers were calibrated before and after the test using a NIST-traceable positive displacement primary piston prover and have an uncertainty of less than 1% full-scale.<sup>21</sup>

All power to the SPT-140 was provided using commercial laboratory power supplies. The discharge was controlled using three 15-kW (1000 V, 15 A) power supplies connected in a master-slave configuration. Circuitry between the laboratory supplies and the thruster was chosen to be representative of the Psyche flight design. The outputs of all supplies were connected to the thruster through the TASU-140. Laboratory wire harness with an inductance and capacitance of approximately 2.5  $\mu\text{H}$  and 236 pF, respectively,<sup>22</sup> completed the power circuit from the TASU to the thruster. The total inductance between the TASU and SPT-140 was measured to be approximately 6.2  $\mu\text{H}$ , which is comparable to the value expected onboard the Psyche spacecraft. The TASU contains the SPT-140 system filter capacitor; the filter inductor normally housed in the PPU was located between the lab supplies and the TASU for this test.

The SPT-140 thruster body was configured to float with respect to facility ground and all conductive surfaces within one meter of the thruster exit plane were insulated using Kapton sheeting. This was done in order to simulate the space electrical environment by minimizing the number of electrical coupling paths between the HET and facility in the near-field.<sup>23,24</sup>

Thruster telemetry and facility pressure were collected continuously at a rate of 1 Hz using a multiplexed data acquisition system and saved to a data file at a rate of  $\sim 0.5$  Hz. End-to-end calibrations of the laboratory power and data acquisition systems were performed before and after the test using a NIST-traceable digital multimeter. The resultant uncertainty was approximately  $\pm 0.06$  V and  $\pm 0.03$  A for measurements of current and voltage, respectively. Discharge current oscillations were measured using a 150-A AC/DC current probe connected to an oscilloscope; oscillations in discharge voltage and cathode-to-ground voltage were measured using high-voltage differential probes connected to the same oscilloscope. All oscillation data were sampled at a rate of 1 MS/s. The root-mean-square (RMS) and peak-to-peak values were computed by the oscilloscope over intervals composed of 100,000 samples and recorded by the data acquisition system. These computed oscillation values were not saved to a data file by the automated data system but rather by manual command when desired by the test operators.

The thrust stand was of the inverted pendulum style and was operated in a null-coil configuration with in-situ calibration. The thrust stand was used most recently for testing of a 12.5-kW Hall thruster and has additionally supported a number of projects in VF-5. Available references<sup>25-27</sup> outline many of the design features and best operating practices used with the thrust stand. The thrust stand used a closed loop differential/integral controller to maintain the position measured by a linear variable differential transformer. Two voice coils provided the actuation for position control, additionally the current through the voice coils served as the measure of thrust. Inclination was tuned with a combination of automated piezoelectric actuator and manual stepper motor on a power screw. The inclination was controlled with a closed loop integral controller to maintain inclination measured by an electrolytic tilt sensor. The thrust stand was calibrated in-situ by applying load to the stand generated from a set of known masses. Thrust uncertainty was determined to be  $\pm 2.1$  mN to  $\pm 2.6$  mN as described in Section III.D.

### C. Test Methods

The SPT-140 manufactured for SSL uses a specific start-up sequence dictated by the SSL PPU with the objective of properly warming-up the electronics and the active elements of the thruster, but also limiting the PPU in-rush currents. The system is nominally started at a discharge power of 3.0 kW and the power is then adjusted to the level of interest after a few minutes. The very first time the thruster is turned on after exposing the unit and the vacuum chamber to atmosphere, the SPT-140 needs to undergo an initial bake-out at a power of 3.0 kW for at least one hour in order to outgas any absorbed moisture.

Even though the tests presented here were not performed with an SSL PPU, the nominal thruster start-up sequence was used. After warming and setting up the power supplies, the start-up sequence consisted of: 1) power the magnet coil up to 4.5 A; 2) power the cathode heater up to 17.3A (note that this value is specific to each cathode); 3) after 150 seconds set the flow rate through the anode and cathode to a total flow rate of about 11 mg/s with a ratio of  $\dot{m}_a : \dot{m}_c = 20:1$ ; 4) turn on the discharge power supply at a set voltage of 300 V; 5) turn on the keeper power supply with

a voltage limit of 320 V and a current limit of 1.15 A; and 6) as soon as the discharge current is at least 4 A the keeper power supply and the cathode heater power supply are turned off.

The thruster was able to start consistently upon application of the keeper voltage. Several seconds were required to reach an equilibrium propellant flow rate and rise to the target power level of 3.0 kW. As this power was approached, the anode and cathode flow rates were manually adjusted to achieve a discharge current of 10 A and a cathode flow fraction of 5%.

In the commercial application, the thruster is allowed to throttle from 3.0 kW to a higher power after operating for a few minutes, which is required to homogeneously distribute the heat across the discharge chamber. The sequence to increase the discharge power is: first, set the magnet current for the new, higher power level; then, adjust the anode and cathode flow rate to reach the required discharge current, while maintaining the cathode flow fraction at 5%. The order of this setting is inverted when the discharge power is lowered: first, adjust the propellant flow rate, while keeping the cathode flow fraction constant; then, set the magnet current according for the lower power level. This specific sequence is preferred because the thruster can experience larger discharge current oscillations, instabilities and even change operation mode if the magnet current is not strong enough for the selected discharge power.<sup>15</sup> Once the target power was reached, the overall system (i.e. thruster and diagnostics) was operated for two hours before collecting data. For subsequent throttle changes after the thruster had been running for hours, a shorter equilibration duration was used that depended on the power level change.

For the initial operation at each power level, a magnet current sweep was performed to verify the magnet current setting. The magnet current setting of the SPT-140 is not a strict requirement, it can be adjusted within a range of a  $\pm 1$ A of the nominal value. The maximum magnet current of the system is limited to 6.5 A, while the minimum is 2.5 A. For this test the magnet current was briefly swept in 0.25 A steps at constant flow rate while monitoring the thruster operation. The magnet current was optimized to minimize the discharge current oscillations (RMS and peak-to-peak values).

The final set points used at each power level for the tests described herein are shown in Table 1. The nominal cathode flow fraction used for all testing was 5%, with the exception of some low-power tests which used flow fractions of 9% and 20% as well. Note this nominal flow fraction is slightly less than the 7-8% used in previous investigations of SPT-140 throttling and low power operation.<sup>6,7</sup>

As discussed in the introduction, the main objective of this test was to investigate the change in thruster performance at different power levels and facility background pressures. Facility pressure was increased above the nominal operating pressure at each power level by injecting gas into the chamber from the downstream facility bleed line. The only limitation on the pressure change was that the minimum bleed flow was about 30 sccm. Performance measurements were obtained at eight to ten different facility pressures ranging up to 20 to 40  $\mu$ Torr. The selected pressures were purposely spaced non-uniformly in order to focus on the trends observed at lower pressures. At least 10 minutes were allowed to elapse to stabilize the thruster after each change in facility pressure. After 10 minutes, if the discharge current was deviating from the nominal value by more than 30 mA or the cathode flow fraction was deviating by more than 0.2%, the propellant flow rate was adjusted. Data were not recorded until stable, nominal operation had been achieved for at least five minutes following any flow rate adjustments. After mapping the whole pressure range by increasing the bleed flow sequentially, the bleed flow was turned off and performance measurements were repeated at the minimum facility background pressure.

At the lowest power of 0.9 kW, the variable pressure testing was performed using two different sets of keeper current and cathode flow fractions. Previous testing has shown that adding keeper current and/or additional cathode propellant flow mitigates the large cathode-to-ground voltages that occur when operating at the nominal high-power flow fraction and no keeper current.<sup>6,7</sup> For this variable pressure test, the thruster was operated at 0.9 kW with (a) the nominal 5% cathode flow fraction and 1.15 A of keeper current, and (b) a 20% cathode flow fraction and no keeper current. The intent was to determine if the thruster performance sensitivity to pressure was significantly different for these two different cathode operating conditions. The variable pressure test was performed as described above, but at each pressure level the two cathode operating conditions were used with a minimum 10-minute interval between

**Table 1. SPT-140 Controlled Parameters for Test.**

Discharge Voltage V	Discharge Current, A	Discharge Power, kW	Magnet Current, A
300	3.00	0.90	2.75
	5.00	1.50	3.25
	6.67	2.00	3.25
	8.33	2.50	4.00
	10.00	3.00	4.50
	11.67	3.50	5.50
	15.00	4.50	6.00

changing operating conditions and recording data. Additionally, at 0.9 kW the thruster discharge became significantly noisier at pressures greater than 10  $\mu$ Torr and the magnet current was increased by up to 0.35 A to counteract this.

An additional set of cathode operating condition tests was performed at the lower power levels and the lowest facility pressure to investigate the effects of added keeper current and cathode flow fraction over a range of conditions. These data were gathered in order to help inform the choice of low-power operating conditions for the thruster during the Psyche mission. Keeper currents of 1.15 to 1.75 A and cathode flow fractions of 5% to 20% were investigated.

Finally, a magnetic field sensitivity test was performed at selected power levels and facility pressures. The objective of this test was to examine the sensitivity of thruster operation to magnetic field at different background pressures. The test was conducted at discharge powers of 0.9, 2.5, and 4.5 kW and at four different pressures ranging from the lowest operating pressure up to about three times that pressure. At each power level, the pressure was set as explained earlier and the magnet current was swept with 0.1 A steps every  $\sim$ 20 seconds at constant propellant flow rate. Although tests at constant discharge current would have been more representative of in-flight operation with the PPU, the manual flow control used here did not make that approach feasible.

The thrust stand was calibrated each day before the test was started and after it was completed. A thrust stand zero measurement was taken immediately before and after each of the pressure sweep tests, with the exception of the pre-test measurement at 1.5 kW which was recorded about an hour prior to the test, and the pre-test measurement at 3.5 kW which was recorded about two hours prior to the test. The inclination of the thrust stand was periodically adjusted as necessary during the testing. Thrust data presented here were corrected for thermal drift using the pre- and post-test zero measurements assuming a linear drift with time. All data points reported here are averages of data collected over steady-state periods of 15 to 120 seconds, with the exception of the RMS and peak-to-peak oscillation data which were single-point captures of values computed by the oscilloscope.

### III. Experimental Results

#### A. Performance Variation with Facility Pressure

Full-power thruster performance data obtained as the facility pressure was varied are shown in Fig. 4. The magnet current was held fixed at 6.0 A as these data were acquired, and the thruster flow rate was varied to keep the discharge current fixed at 15.0 A. The error bars in the figure represent fixed uncertainties of  $\pm 2.5$  mN for thrust and  $\pm 7\%$  for pressure as described in Section III.D. The thrust increase as the pressure was increased was notably larger than the measurement uncertainty. At the lowest pressure of 3.2  $\mu$ Torr the measured thrust was as low as 278.7 mN, and at the highest pressure the thrust was 298.7 mN, an increase of 20 mN (7.2%) over the approximately tenfold increase in pressure. This is a larger performance change than the  $\sim 3\%$  observed in a test of the SPT-100 over a tenfold pressure increase.<sup>8</sup> Note that the two thrust measurements at the lowest pressure were taken just before and just after the measurements with increased facility background pressure and show good repeatability.

A significant finding from this test is that the thrust performance did not show a constant value at the lower pressures, i.e. ‘level off’ as the facility pressure was decreased. This is an indication that if the pressure were to be decreased further than was possible in this test then the thrust might also decrease below the minimum observed here. Although the trend would suggest this, there is not a way to determine it experimentally without improved facility pumping speed. This complicates the prediction of in-space performance and will be discussed later in Section IV.

Typically in this type of test, the thruster mass flow rate required to achieve a fixed discharge current decreases measurably as the facility background pressure increases (or, conversely, the discharge current increases at fixed flow rate).<sup>8-11,13</sup> That was not the case, however, for this SPT-140 test at full power as seen in Fig. 5. Here the

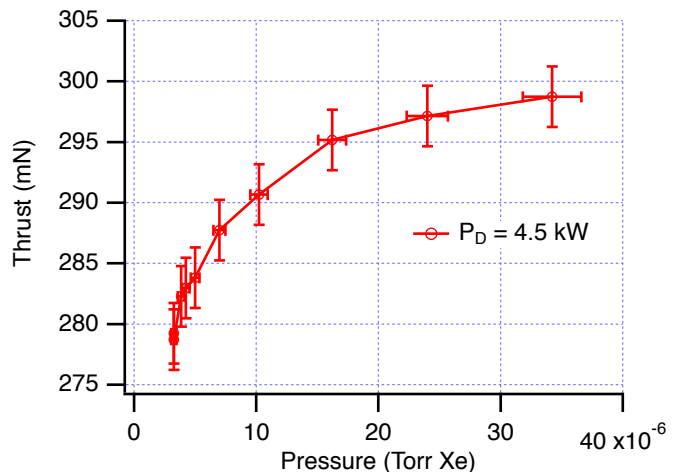


Fig. 4. Thrust Performance at 4.5 kW Discharge Power.

observed flow rate variation was within the  $\pm 1\%$  measurement uncertainty. This was the case for all power levels from 2.5 kW to 4.5 kW.

Discharge and cathode-to-ground RMS oscillations, shown in Fig. 6, were relatively low and did not show large changes as facility pressure varied. The discharge oscillations were only  $\sim 3\%$  and  $\sim 0.3\%$  of the nominal values for current and voltage, respectively. Multiple data points at the lowest pressures are again measurements taken before and after the facility pressure variation.

Thrust data for the other test conditions with discharge power levels of 3.5 kW to 0.9 kW are shown in Fig. 7 through Fig. 12. Note that to facilitate comparison of the data the ranges of the thrust and pressure axes are the same in each figure (i.e. 30 mN range for thrust and 0 to 40  $\mu$ Torr range for pressure). In each case the facility pressure was raised by up to a factor of ten to twenty times above the lowest pressure for the operating condition. Thrust performance did not appear to level off at low pressures in these tests with the exception of the 0.9 kW operating condition where the data scatter and measurement uncertainty preclude this conclusion. Also at 0.9 kW, the thrust measured with steady-state keeper current was slightly lower than for the no-keeper condition at the lowest pressures, although that difference was within the measurement uncertainty.

The data in Fig. 4 and Fig. 7 through Fig. 12 show that the magnitude of the thrust change as pressure was varied decreased as discharge power was decreased, from a 20 mN change at 4.5 kW to 4 mN at 1.5 kW. The relative thrust change is shown in Fig. 13, where the thrust at each pressure and power level was normalized by the lowest thrust measured at that power level. The behavior is

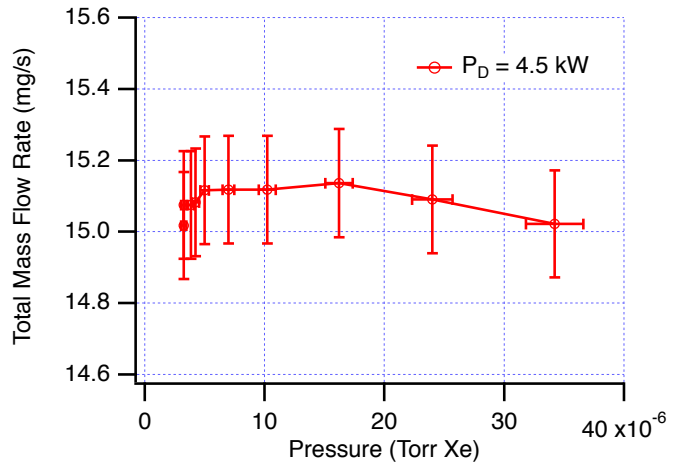


Fig. 5. Thruster Mass Flow Rate at 4.5 kW Discharge Power.

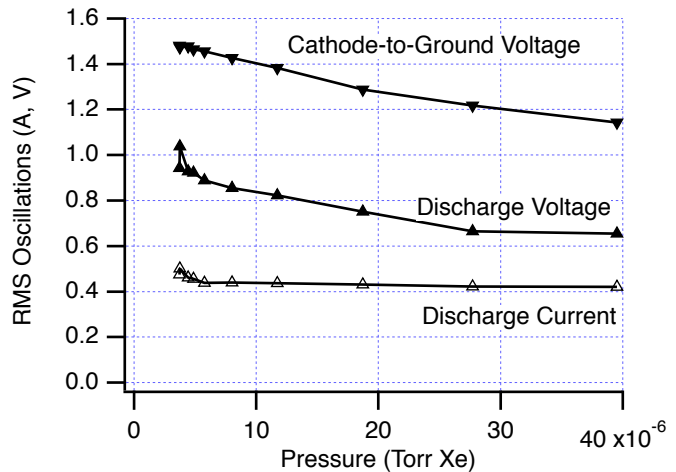


Fig. 6. Discharge and Cathode-to-Ground Voltage Oscillations at 4.5 kW Discharge Power.

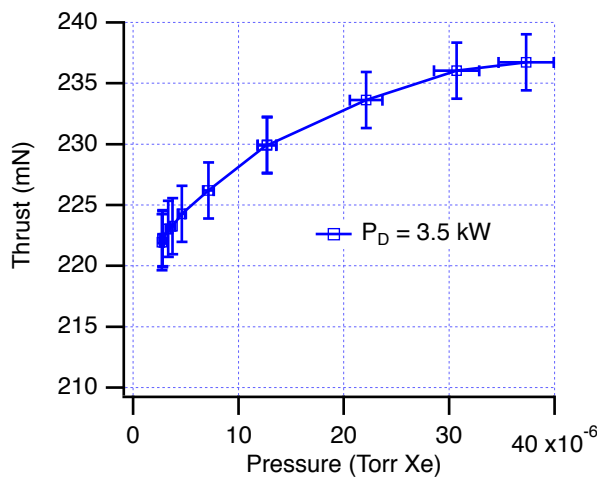


Fig. 7. Thrust Performance at 3.5 kW Discharge Power.

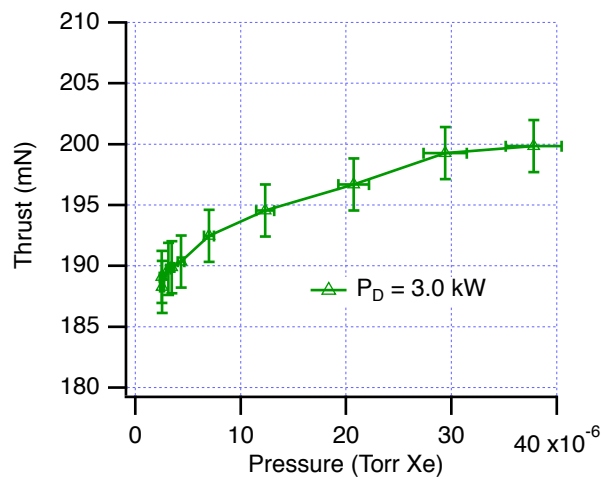


Fig. 8. Thrust Performance at 3.0 kW Discharge Power.

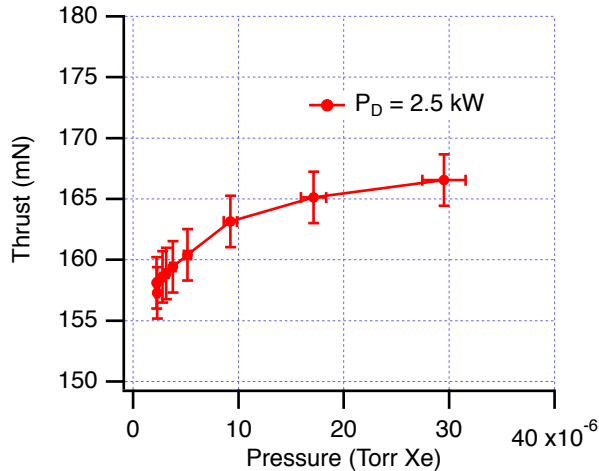


Fig. 9. Thrust Performance at 2.5 kW Discharge Power.

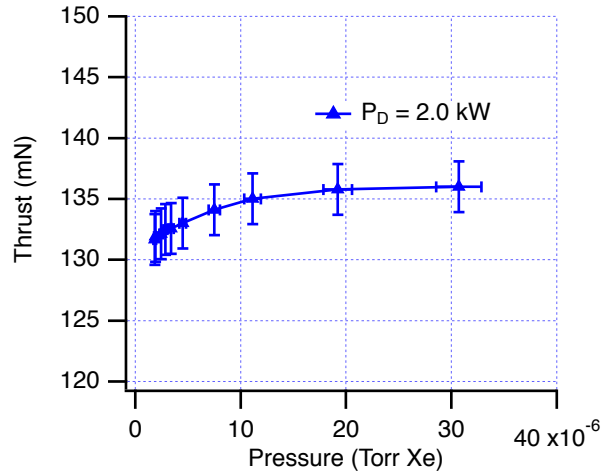


Fig. 10. Thrust Performance at 2.0 kW Discharge Power.

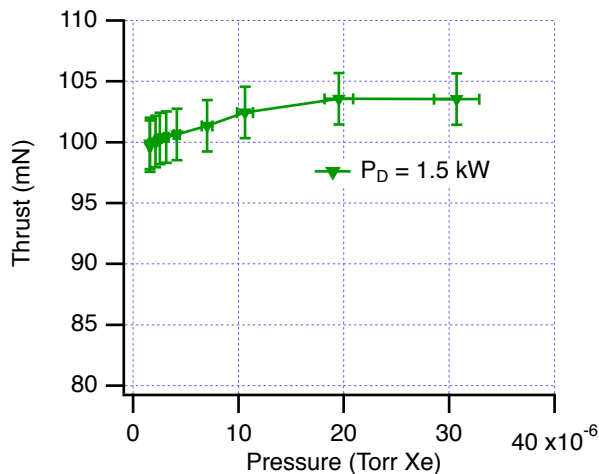


Fig. 11. Thrust Performance at 1.5 kW Discharge Power.

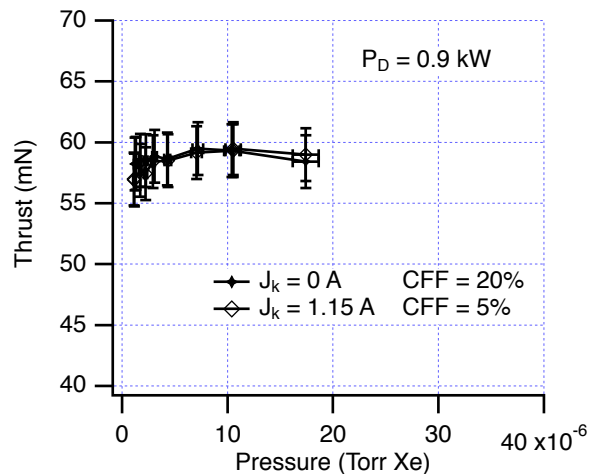


Fig. 12. Thrust Performance at 0.9 kW Discharge Power.

similar for all powers, with a thrust increase of about 2 to 4% at 10  $\mu$ Torr and an increase of about 3 to 7% at the highest pressures tested. The data acquired at 0.9 kW are not shown here; Fig. 12 shows little if any sensitivity to pressure within the measurement error, and that the relative thrust uncertainty is large for that condition.

Recall that the thruster mass flow rate variation as pressure was varied was less than the measurement uncertainty for discharge powers of 2.5 kW to 4.5 kW. At the three lowest power levels there was an observable thruster mass flow rate decrease as facility background pressure was increased, as seen in Fig. 14 for the 1.5 kW condition. The 2.0 kW and 0.9 kW power levels showed similar behavior. Thruster mass flow rate for the 1.5 kW and 2.0 kW power levels was invariant for pressures less than 10  $\mu$ Torr, and only

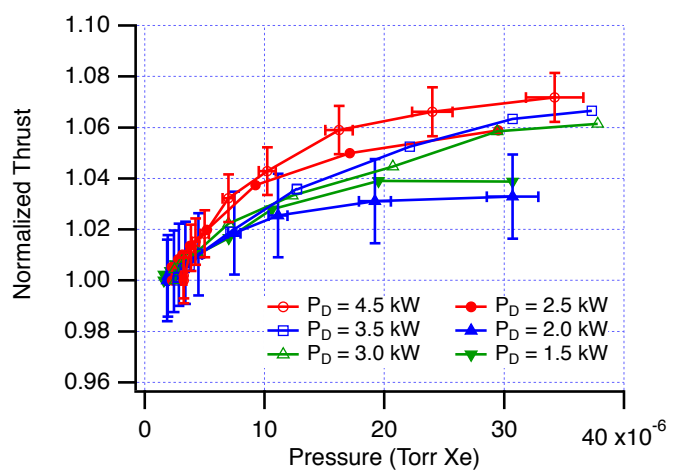


Fig. 13. Normalized Thrust for Discharge Powers of 1.5 to 4.5 kW (to improve readability, only some of the uncertainty bars are included).

a slight change was observed at 0.9 kW for the same pressures.

Discharge current and voltage oscillations for all power levels are shown in Fig. 15 and Fig. 16. The discharge current RMS oscillations were less than 5% of the steady-state discharge current at all powers and do not show large trends with pressure, with the exception of the 0.9 kW case which showed significant increases and which for the no-keeper case were as high as 15% of the mean discharge current. As will be discussed later, however, the latter operating condition is not of interest for the Psyche mission. Discharge voltage oscillations were also small, less than 0.35% of the 300 V nominal operating voltage for all conditions. Both current and voltage show slight *increasing* trends at the higher power levels as pressure was decreased but because the magnitudes are so small this is not a particular concern. This is in contrast to the behavior in some other Hall thruster studies which exhibited *decreasing* discharge current oscillations as pressure was decreased, sometimes significantly, albeit with oscillations larger than observed here (typically a few to 10-20%).<sup>8,9,11</sup> Oscillation behavior with pressure in Hall thrusters is not very well understood and more work on the phenomena is warranted.

Measured thruster operating conditions and performance for the lowest obtainable facility pressures are summarized in Table 2.

## B. Low-Power Operation

As discussed in the introduction, operation of the SPT-140 DM4 at lower powers has been shown to yield increasingly negative cathode-to-ground voltages which can be mitigated by the addition of steady-state cathode keeper current and extra xenon flow to the cathode. A goal of this testing was to examine low-power behavior over a similar range of conditions with a qualification model thruster and to compare to operating conditions used in the low-power life test extension. As anticipated, the low-power cathode-to-ground behavior observed with DM4 was also observed during this test series with the QM002 thruster, as shown in Fig. 17. At discharge powers greater than 1.5 kW, the cathode-to-ground voltage remained within the -17 V to -23 V range observed during the QM001 life test at 3.0 and 4.5 kW. At lower powers, however, this voltage decreased to as much as -35 V. Addition of 1.15 A of steady-state keeper current raised the cathode-to-ground voltage by about 4.5 V at the lowest power. Although this was a reasonable increase, it still yielded a voltage that was

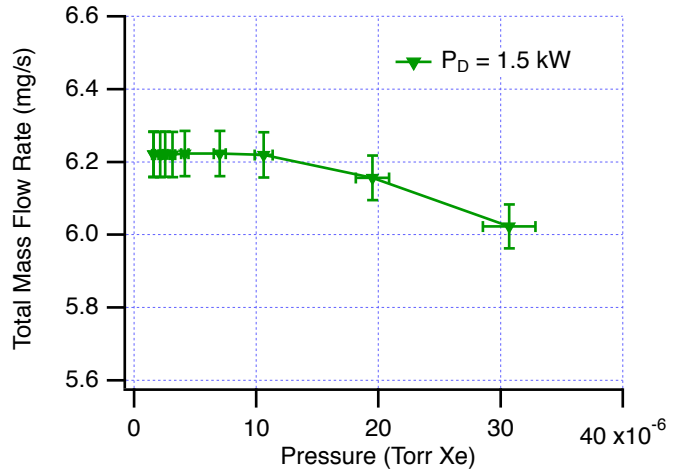


Fig. 14. Thruster Mass Flow Rate at 1.5 kW Discharge Power.

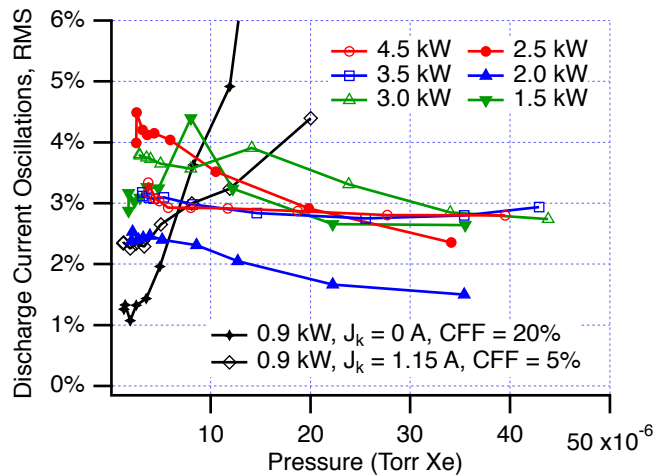


Fig. 15. Normalized Discharge Current Oscillations for All Power Levels.

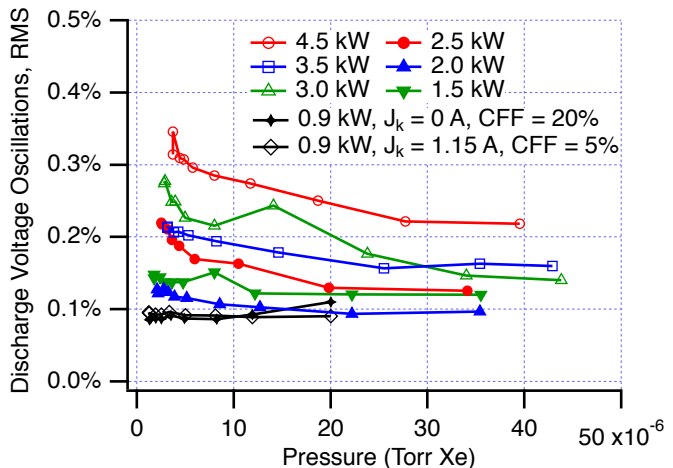


Fig. 16. Normalized Discharge Voltage Oscillations for All Power Levels.

**Table 2. Thruster Operating Conditions and Performance Measured at Lowest Background Pressures.**

Discharge Current, A	Discharge Voltage, V	Magnet Current, A	Total Flow Rate, mg/s	Cathode Flow Fraction*	Keeper Current, A	Cathode-to-Ground Voltage, V	Total Thruster Power, kW	Thrust, mN	Specific Impulse, sec	Thruster Efficiency	Tank Pressure, Torr Xe
14.98	299.6	6.00	15.9	5.0%	0	-20.4	4.57	279.3	1794	53.7%	3.25E-06
11.67	300.0	5.52	13.0	5.0%	0	-21.2	3.58	222.0	1739	52.9%	2.78E-06
9.99	300.2	4.53	11.3	5.0%	0	-19.9	3.05	189.1	1710	52.1%	2.51E-06
8.32	300.3	4.00	9.7	5.0%	0	-19.9	2.53	158.1	1662	50.9%	2.22E-06
6.66	300.5	3.25	8.3	5.0%	0	-20.6	2.02	131.7	1627	52.0%	1.84E-06
4.98	300.7	3.24	6.6	5.0%	0	-24.4	1.52	99.7	1545	49.8%	1.57E-06
2.97	300.8	2.75	4.1	5.0%	1.15	-30.4	0.93	57.0	1400	42.1%	1.15E-06
2.99	300.9	2.76	4.3	9.0%	1.15	-26.0	0.93	57.1	1364	40.9%	1.11E-06
3.00	300.9	2.75	4.6	20.0%	0	-26.7	0.91	58.2	1283	40.0%	1.20E-06

\* Cathode Flow Fraction is defined as cathode flow rate divided by anode flow rate.

significantly more negative than at full power. If maintaining the cathode-to-ground voltage near the full-power value is the goal, adding keeper current alone is insufficient at the lowest powers.

The effects of both keeper current and added cathode flow are shown together for the lowest discharge power of 0.9 kW in Fig. 18. Addition of cathode flow up to a flow fraction of 20% without keeper current increased the cathode-to-ground voltage by 8 V to -27 V. Alternatively, addition of a keeper current of 1.75 A (i.e. about the maximum allowable keeper power) with no added cathode flow raised the cathode-to-ground voltage a similar amount. Addition of cathode flow rate clearly has diminishing returns, while the effect of adding keeper current is nearly linear. Also clear is that it would be difficult and likely prohibitive with this system design to levy a requirement that the cathode-to-ground voltage be nearly constant at a value of -20 V to -22 V across all discharge powers.

For the SPT-140 life test extension at low discharge powers, a cathode flow fraction of 9% and a keeper current of 1.15 A were chosen.<sup>4</sup> As seen in Fig. 18, this operating condition captures the majority of the possible gains in cathode-to-ground voltage with modest increases in keeper current and cathode flow fraction. Over the course of the QM001 life test, cathode-to-ground voltages of -17 V to -23 V were observed at the discharge powers of 3.0 and 4.5 kW. The life test extension, which was performed at 0.9 kW for 250 hours and 1.0 kW for 250 hours, demonstrated slightly lower cathode-to-ground voltages of -23 V to -24.5 V, which are not a significant departure from the full-power values.

Discharge current oscillations were also monitored as keeper current and flow fraction were varied. Those results are shown in Fig. 19. Current oscillations decreased slightly as cathode flow fraction was increased, and the additional keeper current had no effect with the exception of a slight increase at 9% flow fraction. Discharge voltage and

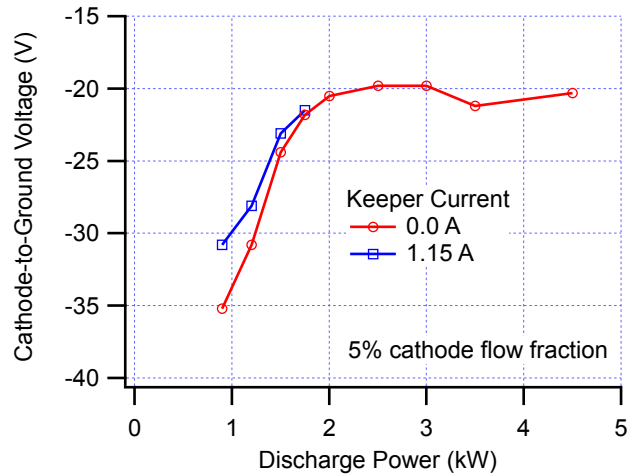


**Fig. 17. Cathode-to-Ground Voltage Behavior at 5% Cathode Flow Fraction.**

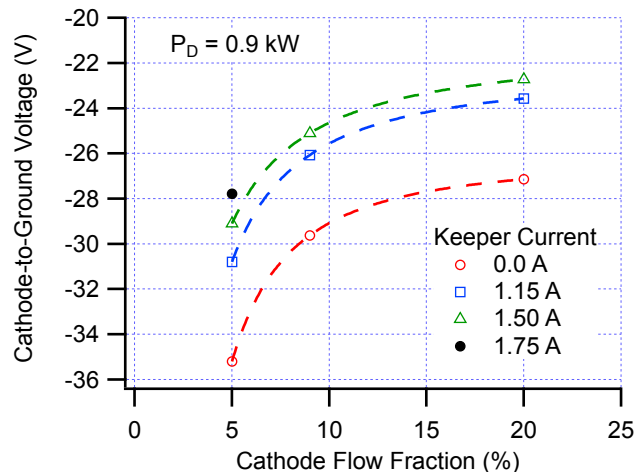


**Fig. 18. Effect of Added Cathode Keeper Current and Flow Rate on Cathode-to-Ground Voltage.**

cathode-to-ground voltage oscillations also showed little-to-no dependence on these two parameters.

### C. Magnetic Field Sensitivity

In Section III.A the thruster performance sensitivity to background pressure was presented. Since a significant pressure dependence was observed, the sensitivity of thruster behavior to magnetic field at different pressures was also of interest. These effects were measured at three thruster powers spanning the range tested here (0.9, 2.5, and 4.5 kW), and at four different pressures from the lowest operating pressure up to about three times that pressure. At 0.9 kW both cathode operating conditions of (a) the nominal 5% cathode flow fraction and 1.15 A of keeper current, and (b) a 20% cathode flow fraction and no keeper current, were examined.

For the most part, the results obtained during this set of tests showed no significant dependence on pressure. This included thrust, cathode-to-ground voltage, and cathode-to-ground voltage oscillations at all operating conditions. An example of the lack of dependence on pressure is shown in Fig. 20 for discharge current oscillations at a power of 2.5 kW. The oscillations increased as the magnet current was varied below and above the set point at a given pressure, but it can be seen that the magnitude of the oscillations at each magnet current did not depend appreciably on the facility pressure. (Most results showed even less variation with pressure than this one).

The discharge current did show an interesting dependence on pressure at 4.5 kW, as shown in Fig. 21. Because the propellant flow rate was fixed in this test, the discharge current varied with magnet current, and it can be seen that the slope of the curve near 6 A became less steep as pressure was increased. In this mode of operation, lower pressures appear to increase the sensitivity of discharge current to magnet current variations over the range of 5.75 to 6.5 A.

In tandem with the discharge current sensitivity, the discharge current oscillation sensitivity at 4.5 kW depended on pressure as shown in Fig. 22. Here the oscillations were about the same level at the minimum and maximum magnet currents, but the curve became steeper and the threshold for increase closer to 6 A at lower pressures. Although these two figures might suggest the choice of a higher magnet current for the 4.5 kW operating point, recall that the PPU will control the discharge current at a constant value and so the in-flight behavior would be different as magnet current is varied. Also note that the increase in discharge

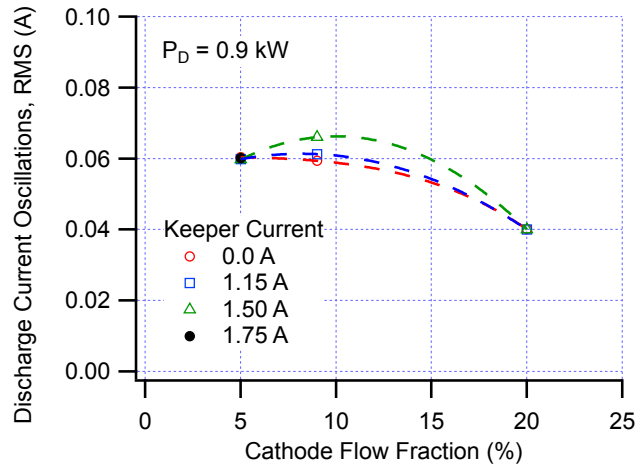


Fig. 19. Effect of Added Cathode Keeper Current and Flow Rate on Discharge Current Oscillations.

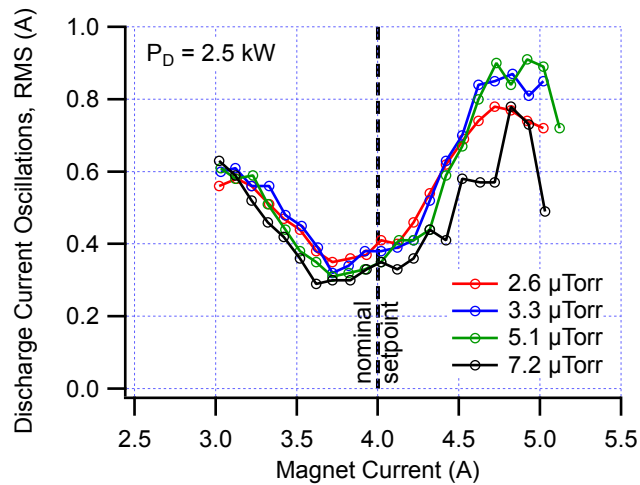


Fig. 20. Discharge Current Oscillation Sensitivity to Magnet Current and Pressure at 2.5 kW.

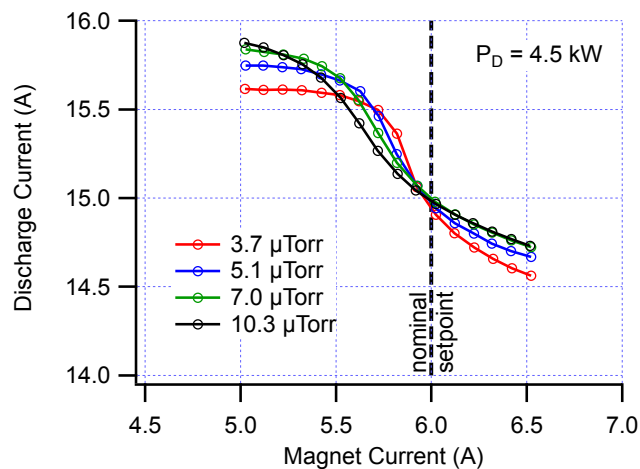


Fig. 21. Discharge Current Sensitivity to Magnet Current and Pressure at 4.5 kW.

current oscillations from high to low magnet currents in Fig. 22 is from 3% to 6% of the mean discharge current, which is a small fraction.

At the lower powers of 0.9 and 2.5 kW the discharge current and current oscillation variation with magnet current showed no significant dependence on pressure. A slight dependence of current oscillations was observed at 0.9 kW, however, and it is interesting to compare the results for the two different operating conditions, shown in Fig. 23. Both operating conditions show a slight decrease in current oscillations with decreasing pressure at many magnet currents. Also noteworthy is that the operating condition with keeper current does not show the same sensitivity to magnet current as does the condition without keeper current. In either case the current oscillations are less than 10% of the mean discharge current at nearly all magnet currents investigated.

## D. Measurement Uncertainties

### 1. Pressure Measurement

As recommended in both the ASTM standard for ionization gauge operation and the AIAA guidelines for pressure measurement in electric propulsion testing, in order to minimize uncertainty, the acquired pressure measurements were corrected for both gauge temperature and calibration.<sup>20,28</sup> The impact of gauge temperature on the acquired pressure measurements can be described by Eq. (1), where  $P_{gas}$  is the corrected pressure,  $P_{gauge}$  is the uncorrected pressure,  $T_{gas}$  is the temperature of the ambient gas,  $T_{gauge}$  is the temperature of the ionization gauge walls, and all  $cal$  values correspond to those measured during calibration of the gauge.<sup>20,28</sup> During calibration, the temperature of the gas and gauge were measured to be approximately 23°C and 50°C, respectively. During operation in VF-5, measurements have shown an average gauge temperature of approximately 13°C and the gas temperature is assumed to be equal to the measured facility wall temperature of approximately 23°C. Substituting these values into Eq. (1) yields an average thermal correction factor of approximately 0.94.

$$P_{gas} = P_{gauge} \sqrt{\frac{T_{gas} T_{gauge}}{T_{gas cal} T_{gauge cal}}} \quad (1)$$

The gauges used in this work were calibrated as an end-to-end system using a NIST-referenced spinning rotor gauge with xenon gas. The results from this calibration define a piecewise linear calibration curve that can be used to convert an indicated pressure into a corresponding true pressure. For all conditions at which data were recorded, the uncorrected pressure measurement was first corrected for thermal effects using Eq. (1). The thermally-corrected data were then corrected for the gauge calibration using the piecewise linear calibration curve.

The individual uncertainties associated with these correction factors must be propagated in order to determine the overall uncertainty of the reported pressure measurements. As documented in the gauge calibration sheets, the 95% confidence interval uncertainty for the gauge system calibration over the range of pressures of interest for this work

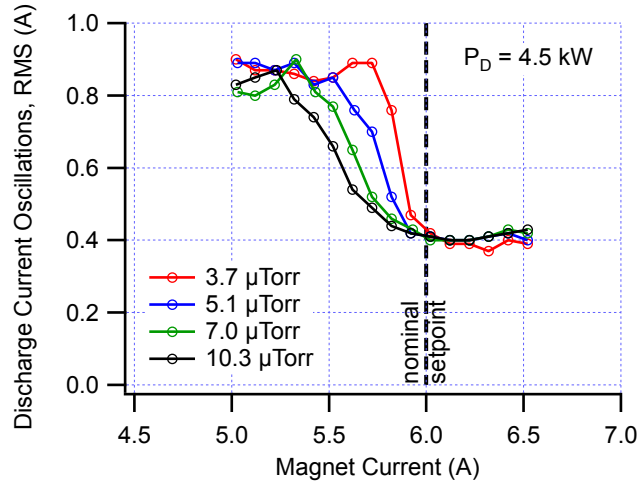


**Fig. 22. Discharge Current Oscillation Sensitivity to Magnet Current and Pressure at 4.5 kW.**

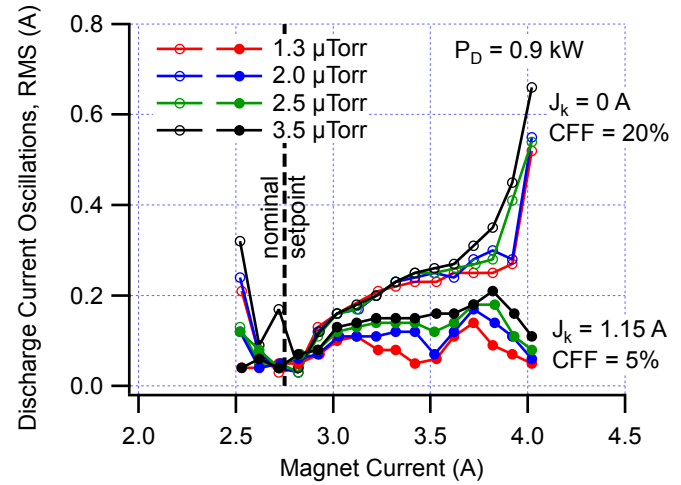


**Fig. 23. Discharge Current Oscillation Sensitivity to Magnet Current and Pressure at 0.9 kW.**

is approximately 7.1%. This represents the remaining uncertainty even after applying the calibration correction. Per the manufacturer specifications, the uncertainty associated with the type K thermocouple measurements used to compute the thermal correction factor is approximately  $\pm 2.2^\circ\text{C}$ . Combining these uncertainties yields a total uncertainty of approximately  $\pm 7.3\%$  for all reported pressure measurements.

## 2. Thrust Measurement

Because the method and details used to quantify the thrust uncertainty are found in the literature,<sup>29</sup> only an abbreviated overview of the method will be presented here. To perform the analysis the stand was modeled as a nominal one degree of freedom four-bar linkage with inherent stiffness and viscous damping elements. The thrust stand was investigated under two operating modes: calibration, and thruster operation. Several sources of uncertainty have been estimated including: DAQ resolution, calibration mass variability, calibration system alignment, calibration pulley moment, gravity uncertainty, inclinometer control resolution, null-coil control resolution, thruster alignment, and calibration regression statistics. Sources of uncertainty were propagated using a truncated Taylor series expansion and combined using an RSS style inner product generated norm. Parameters typical for the SPT-140 testing of this work were used in the calculation including among others the thruster mass, stand natural frequency, and typical calibration regression statistics. For parameters that could not be estimated for this work directly the default choice was to use existing estimations for the VF-5 thrust stand during recent operation with a 12.5 kW Hall thruster.<sup>29</sup> Thrust uncertainty was estimated over a range of nominal thrust levels from 25 mN to 300 mN and was found to range from an uncertainty of  $\pm 2.1$  mN to  $\pm 2.6$  mN.

## IV. Discussion

The main motivation for this work was to understand the dependence of the SPT-140 performance on facility background pressure at a range of power levels and to use that information to develop better performance models for Psyche mission design and trajectory analysis. Thruster performance models used to date have relied on data acquired with the DM4 thruster<sup>6</sup> and corrections for background pressure based on the unpublished results of tests at powers of 3.0 and 4.5 kW with QM002 (the tests were similar to those described in Ref. 8). A critical focus of this series of tests was to determine the pressure dependence at powers less than 3.0 kW.

The results presented here show that the greatest dependence of performance on pressure occurred at the highest power level of 4.5 kW, both in an absolute and in a relative amount. Although the absolute dependence on pressure decreased with power, the relative levels were similar for discharge powers larger than 1 kW (see Fig. 13). At the lowest power level there was essentially no dependence on pressure within the measurement uncertainty. The thruster performance models developed prior to this test had assumed similar behavior, so these test results validated that set of assumptions, at least with respect to the range of pressures investigated here.

Although the electric propulsion community has performed many studies of pressure effects on Hall thruster performance, there is not yet a good physics-based model that describes the effects observed here in a way that can be used to predict performance in space (see for example Reference 11 and references therein). SSL has successfully used an empirical model to correct for pressure effects on its satellites with the SPT-100 system, but the thrust uncertainties associated with this type of method will likely be larger for the SPT-140. For example, extrapolation of the 4.5 kW thrust data to zero pressure could lead to thrust predictions as high as 278 mN or as low as 260 mN or lower depending on the assumptions used. Ideally this phenomenon would be described with physics-based models that can be used with confidence to predict in-space performance. In lieu of that, one solution could be to extrapolate performance conservatively and add margin into the performance model. As a preliminary step to understand the sensitivity of the baseline Psyche trajectory<sup>1</sup> to thrust, the trajectory was re-analyzed using a very conservative thruster performance (e.g. 250 mN at 4.5 kW). For this case, the arrival date and propellant consumption were similar but the delivered mass to asteroid capture decreased by almost 2%. This is not an insignificant amount, but the mission has ample mass margin and the trajectory does appear to be robust to drastic thruster underperformance. Prediction of in-space performance is an area that needs more work, and this will be aided by data gathered during the planned multiple flights of the SPT-140 system on SSL commercial spacecraft prior to the launch of the Psyche spacecraft.

A secondary motivation for this work was to gather additional data on low-power operation to inform the selection of mission operating conditions and revision of hardware performance requirements where necessary. Thruster operation at powers of 0.8-1.0 kW has shown to be stable and repeatable, with the only appreciable concern being the relatively large cathode-to-ground voltages that have been observed at low discharge currents and low cathode flow

rates. These large voltages are likely required to provide the ion heating from a higher cathode sheath voltage necessary to maintain the required insert temperature for discharge current emission. There is no hard criterion for an acceptable value of cathode-to-ground voltage, but basic knowledge of cathode physics suggests that too large of a value could impact the cathode health and life.<sup>15</sup> An excessively large value would also affect overall thrust performance. Note that the life test of the SPT-140 was conducted with cathode-to-ground voltages in the range of -17 V to -24.5 V.

The data obtained in this test series indicate that a combination of keeper current and additional cathode flow is more effective in raising the cathode-to-ground voltage than using either one alone (see Fig. 18). In fact, the addition of a modest keeper current of 1.15 A and cathode flow fraction of 9% (i.e. the values used in the SPT-140 low-power life test extension) reduced the cathode-to-ground voltage to a value close to that observed over the duration of the life test. It also increased the thrust by 3%. These cathode operating conditions have now been baselined for low-power operation during the Psyche mission. Impacts to the electric propulsion subsystem<sup>4</sup> include redesign of the PPU-140 ignitor power supply to allow steady-state keeper current, and addition of an extra valve and flow control orifice to the XFC to allow for extra propellant to the cathode at low power. Impacts to the spacecraft include the additional power consumption (~23 W of keeper power) and additional propellant (~1 kg for the entire proximity operations phase).

The present mission design calls for 1500 hours of low-power electric propulsion system operation at the asteroid (see Fig. 1). With four thrusters on the spacecraft and a requirement for single-fault tolerance, that operating time can be spread among three thrusters. This means that the SPT-140 qualification model life test has already demonstrated the required operating time (500 hours) at low power required by the mission. Note that the low-power operation extension was conducted after the thruster had been operated at 3.0 kW and 4.5 kW for a throughput of 470 kg,<sup>4</sup> analogous to the Psyche usage where low-power operation will be conducted after the long-duration heliocentric cruise.

Other items of interest for the SPT-140 subsystem as the Psyche development continues include development of a startup sequence to allow for startups at powers less than 3 kW, design of the specific XFC architecture for additional cathode flow at low powers, selection and validation of magnet currents for operation at each power level, and validation of thruster lifetime for the Psyche throttle profile using model simulations.

## V. Conclusion

Performance of the SPT-140 Qualification Model 002 was investigated as a function of facility background pressure over a discharge power range of 0.9 kW to 4.5 kW. The absolute thrust dependence on pressure was largest at the highest power and decreased as power decreased, to a point where there was little-to-no measurable dependence at the lowest power. The relative change of thrust with pressure, however, was consistent for all powers above 1 kW at about 2-4% higher thrust at 10  $\mu$ Torr compared to the lowest facility pressure at each power level. Discharge oscillations were relatively small at less than 5% and 0.3% of the mean values, respectively, for current and voltage across all operating conditions and pressures of interest. The data collected will be used to develop updated thruster performance models for mission design and trajectory analysis for the Psyche mission.

Operation of the thruster was also investigated at different cathode operating conditions at 0.9 kW, specifically to determine the effect of cathode keeper current and cathode flow rate on the cathode-to-ground voltage. At the nominal high-power conditions of no keeper current and 5% flow fraction, the cathode-to-ground voltage became increasingly negative at lower powers, and this was mitigated by the addition of keeper current and additional cathode flow rate. Neither method used alone, however, was able to produce a cathode-to-ground voltage similar to that measured at higher powers here or in the SPT-140 QM001 thruster life test. It was found that a combination of keeper current and additional flow gave better results, and that values of 1.15 A and 9% flow fraction, respectively, captured the bulk of the benefits. These values have been chosen as the baseline low-power operating condition for the Psyche mission, and they necessitate minor hardware and system architecture changes from the standard commercial implementation of the SPT-140 system.

Finally, a series of tests was performed to determine if the thruster performance sensitivity to magnetic field depended on background facility pressure. Measurements were performed at 0.9, 2.5, and 4.5 kW, and no major sensitivity to background pressure was observed. There was some small but measurable dependence on pressure observed at 4.5 kW in the discharge current and discharge current oscillations, but little if any dependence at the two lower powers. Based on these results, this does not appear to be a significant concern for characterization of thrusters in ground test facilities as compared to operation in space.

## Acknowledgments

The work described in this paper was carried out by the Jet Propulsion Laboratory, California Institute of Technology, under a contract with the National Aeronautics and Space Administration, and by Psyche mission partners SSL and NASA GRC. The authors would like to thank Hani Kamhawi, Peter Peterson, Dave Jacobson, Carol Tolbert, Jeff Woytach, Taylor Seablom, Chad Joppeck, Luke Sorrelle, Richard Senyitko, Nick Lalli, Michael Depauw, James Zakany, and Sandra M. Doehne of NASA Glenn Research Center for their assistance with the planning and execution of this test. The authors would also like to give a special thank you to Kevin L. Blake, George P. Jacynycz, Thomas A. Ralys, Josh Gibson, Jim Szelagowski, and all of the members of the Space Environments Test Branch for assembly of the test setup and operation of the vacuum facility. Thanks to Jason Esquivias, Anthony Nguyen and Samuel Salinas of SSL for supporting the preparation of the test units, to Dan Goebel, David Oh, and Rich Hofer of JPL for their contributions to the development of the test plan, and to Greg Whiffen of JPL for trajectory sensitivity analysis. And finally another thanks to Dan Goebel for traveling to participate in and collaborate on the low-power testing.

## References

1. Oh, D.Y., S.M. Collins, D.M. Goebel, W. Hart, G. Lantoine, J.S. Snyder, G.J. Whiffen, L. Elkins-Tanton, P. Lord, Z. Pirkl, and L. Rotlisburger, "Development of the Psyche Mission for NASA's Discovery Program," IEPC 2017-153, 35th International Electric Propulsion Conference, Atlanta, GA, Oct. 8-12, 2017.
2. Hart, W., G.M. Brown, S.M. Collins, M. De Soria-Santacruz Pich, P. Fieseler, D.M. Goebel, D. Marsh, D.Y. Oh, J.S. Snyder, N. Warner, G.J. Whiffen, L. Elkins-Tanton, J.F. Bell III, D.J. Lawrence, P. Lord, and Z. Pirkl, "Overview of the Spacecraft Design for the Psyche Mission Concept," IEEE Aerospace Conference, Big Sky, Montana, Mar. 3-10, 2018.
3. Delgado, J.J., J.A. Baldwin, and R.L. Corey, "Space Systems Loral Electric Propulsion Subsystem: 10 Years of On-Orbit Operation," IEPC 2015-04, 34th International Electric Propulsion Conference, Kobe, Japan, July 6-10, 2015.
4. Jameson-Silva, K., J.J. Delgado, R. Liang, P.W. Lord, L. Rotlisburger, M. Torres, B. Tomescu, S.P. Malone, E. Werner, and J. Waranauskas, "Adaptability of the SSL Electric Propulsion-140 Subsystem for use on a NASA Discovery Class Missions: Psyche," IEPC 2017-181, 35th International Electric Propulsion Conference, Atlanta, GA, Oct. 8-12, 2017.
5. Delgado, J.J., R.L. Corey, V.M. Murashko, A.I. Koryakin, and S.Y. Pridannikov, "Qualification of the SPT-140 for use on Western Spacecraft," AIAA 2014-3606, 50th Joint Propulsion Conference, Cleveland, OH, July 28-30, 2014.
6. Snyder, J.S. and R.R. Hofer, "Throttled Performance of the SPT-140 Hall Thruster," AIAA 2014-3816, 50th Joint Propulsion Conference, Cleveland, OH, July 28-30, 2014.
7. Garner, C.E., B.A. Jorns, S. van Derventer, R.R. Hofer, R. Rickard, R. Liang, and J.J. Delgado, "Low-Power Operation and Plasma Characterization of a Qualification Model SPT-140 Hall Thruster for NASA Science Missions," AIAA 2015-3720, 51st Joint Propulsion Conference, Orlando, FL, July 27-29, 2015.
8. Diamant, K.D., R. Liang, and R.L. Corey, "The Effect of Background Pressure on SPT-100 Hall Thruster Performance," AIAA 2014-3710, 50th Joint Propulsion Conference, Cleveland, OH, July 28-30, 2014.
9. Kamhawi, H., W. Huang, T.W. Haag, J. Yim, D.A. Herman, P.Y. Peterson, G. Williams, J. Gilland, R.R. Hofer, and I.G. Mikellides, "Performance, Facility Pressure Effects, and Stability Characterization Tests of NASA's Hall Effect Rocket with Magnetic Shielding Thruster," AIAA 2016-4826, 52nd Joint Propulsion Conference, Salt Lake City, UT, July 25-27, 2016.
10. Huang, W., H. Kamhawi, and T.W. Haag, "Effect of Background Pressure on the Performance and Plume of the HiVHAc Hall Thruster," IEPC 2013-058, 33rd International Electric Propulsion Conference, Washington, DC, Oct. 6-10, 2013.
11. Hofer, R.R. and J.R. Anderson, "Finite Pressure Effects in Magnetically Shielded Hall Thrusters," AIAA 2014-3709, 50th Joint Propulsion Conference, Cleveland, OH, July 28-30, 2014.
12. Byers, D. and J.W. Dankanich, "A Review of Facility Effects on Hall Effect Thrusters," IEPC 2009-076, 31st International Electric Propulsion Conference, Ann Arbor, MI, Sept. 20-24, 2009.
13. Diamant, K.D., R. Spektor, E.J. Beiting, J.A. Young, and T.J. Curtiss, "The Effects of Background Pressure on Hall Thruster Operation," AIAA 2012-3735, 48th Joint Propulsion Conference, Atlanta, GA, July 30 - Aug. 1, 2012.
14. Corey, R.L., N. Gascon, J.J. Delgado, G. Gaeta, S. Munir, and J. Lin, "Performance and Evolution of Stationary Plasma Thruster Electric Propulsion for Large Communications Satellites," AIAA 2010-8688, 28th AIAA International Communications Satellite Systems Conference, Anaheim, CA, Aug. 30 - Sept. 2, 2010.
15. Goebel, D.M. and I. Katz, *Fundamentals of Electric Propulsion*. JPL Space Science and Technology Series, ed. J.H. Yuen. Vol. 1. 2008, Hoboken, NJ: John Wiley & Sons, Inc.

16. Lobo, M.J., NASA Glenn Research Center, *Electric Propulsion Laboratory*. Available from: <https://www1.grc.nasa.gov/facilities/epl/> [Cited Dec. 20, 2017].
17. Yim, J.T., D.A. Herman, and J.M. Burt, *Modeling Analysis for NASA GRC Vacuum Facility 5 Upgrade*, NASA TM-2013-216496, 2013.
18. Yim, J.T. and J.M. Burt, "Characterization of Vacuum Facility Background Gas Through Simulation and Considerations for Electric Propulsion Ground Testing," AIAA 2015-3825, 51st Joint Propulsion Conference, Orlando, FL, July 27-29, 2015.
19. Huang, W., H. Kamhawi, T.W. Haag, A. Lopez Ortega, and I.G. Mikellides, "Facility Effect Characterization Test of NASA's HERMeS Hall Thruster," AIAA 2016-4828, 52nd Joint Propulsion Conference, Salt Lake City, UT, July 25-27, 2016.
20. Dankanich, J.W., M.L.R. Walker, M.W. Swiatek, and J.T. Yim, "Recommended Practice for Pressure Measurement and Calculation of Effective Pumping Speed in Electric Propulsion Testing," *Journal of Propulsion and Power*, 2017. **33**(3): p. 668-680, DOI: 10.2514/1.B35478.
21. Snyder, J.S., J.A. Baldwin, J.D. Frieman, M.L.R. Walker, N.S. Hicks, K.A. Polzin, and J.T. Singleton, "Recommended Practice for Flow Control and Measurement in Electric Propulsion Testing," *Journal of Propulsion and Power*, 2017. **33**(3): p. 556-565, DOI: 10.2514/1.B35644.
22. Pinero, L.R., "The Impact of Harness Impedance on Hall Thruster Discharge Oscillations," IEPC 2017-023, 35th International Electric Propulsion Conference, Atlanta, GA, Oct. 8-12, 2017.
23. Peterson, P.Y., H. Kamhawi, W. Huang, J.T. Yim, D.A. Herman, G. Williams, J. Gilland, and R.R. Hofer, "NASA HERMeS Hall Thruster Electrical Configuration Characterization," AIAA 2016-5027, 52nd Joint Propulsion Conference, Salt Lake City, UT, July 25-27, 2016.
24. Frieman, J.D., S.T. King, M.L.R. Walker, V. Khayms, and D.Q. King, "Role of a Conducting Vacuum Chamber in the Hall Effect Thruster Electrical Circuit," *Journal of Propulsion and Power*, 2014. **30**(6): p. 1471-1479, DOI: 10.2514/1.B35308.
25. Haag, T.W., "Thrust Stand for High-Power Electric Propulsion Devices," *Review of Scientific Instruments*, 1991. **62**(5): p. 1186-1191, DOI: 10.1063/1.1141998.
26. Xu, K.G. and M.L.R. Walker, "High-Power, Null-Type, Inverted Pendulum Thrust Stand," *Review of Scientific Instruments*, 2009. **80**(5): p. 055103, DOI: 10.1063/1.3125626.
27. Polk, J.E., A. Pancotti, T.W. Haag, S. King, M.L.R. Walker, J. Blakely, and J. Ziemer, "Recommended Practices in Thrust Measurements," IEPC 2013-440, 33rd International Electric Propulsion Conference, Washington, DC, Oct. 6-10, 2013.
28. ASTM, *Standard Practice for Ionization Gage Application to Space Simulators*, E296-70(2015), ASTM International, West Conshohocken, PA, 2015.
29. Mackey, J.A., T.W. Haag, P.Y. Peterson, and H. Kamhawi, "Uncertainty in Inverted Pendulum Thrust Measurements," to be presented at the 54th Joint Propulsion Conference, Cincinnati, OH, July 9-11, 2018.